

# Net-charge probability distributions in heavy ion collisions at chemical freeze-out

P. Braun-Munzinger<sup>a,b,c,d</sup>, B. Friman<sup>a</sup>, F. Karsch<sup>e,f</sup>,  
K. Redlich<sup>g,a,b</sup>, and V. Skokov<sup>e</sup>

<sup>a</sup>*GSI Helmholtzzentrum für Schwerionenforschung, D-64291 Darmstadt, Germany*

<sup>b</sup>*ExtreMe Matter Institute EMMI, GSI, D-64291 Darmstadt, Germany*

<sup>c</sup>*Technical University Darmstadt, D-64289 Darmstadt, Germany*

<sup>d</sup>*Frankfurt Institute for Advanced Studies, J.W. Goethe University, D-60438 Frankfurt, Germany*

<sup>e</sup>*Physics Dept., Brookhaven National Laboratory Upton, NY-11973, USA*

<sup>f</sup>*Fakultät für Physik, Universität Bielefeld, D-33501 Bielefeld, Germany*

<sup>g</sup>*Institute for Theoretical Physics, University of Wrocław, 50-204 Wrocław, Poland*

---

## Abstract

We explore net charge probability distributions in heavy ion collisions within the hadron resonance gas model. The distributions for strangeness, electric charge and baryon number are derived. We show that, within this model, net charge probability distributions and the resulting fluctuations can be computed directly from the measured yields of charged and multi-charged hadrons. The influence of multi-charged particles and quantum statistics on the shape of the distribution is examined. We discuss the properties of the net proton distribution along the chemical freeze-out line. The model results presented here can be compared with data at RHIC energies and at the LHC to possibly search for the relation between chemical freeze-out and QCD cross-over lines in heavy ion collisions.

*Key words:* Heavy ion collisions, QCD phase diagram, Chiral symmetry breaking, Fluctuations

*PACS:* 12.39.Fe, 11.15.Pg, 21.65.Qr

---

## 1 Introduction

Detailed studies of hadron production in nucleus-nucleus collisions from SIS up to LHC energies provide the very interesting result that particle yields

exhibit thermal characteristics and are well described by the statistical operator of a hadron resonance gas (HRG) [1,2,3]. Furthermore, there is a unique relation between the collision energy and the corresponding thermal parameters, which defines the so called chemical freeze-out line in the temperature and chemical potential  $(T, \mu)$ -plane [1,2,4,5]. The phenomenological freeze-out curve, along which particle yields attain their measured values, is considered to be indicative for the QCD phase boundary.

Moreover, results of lattice QCD studies on the critical temperature  $T_c$  at vanishing chemical potential [6,7] and on the slope parameter characterizing the dependence of  $T_c$  on  $\mu$  [8,9] show that, at high energies, the chemical freeze-out curve is very close to the QCD (cross-over) phase transition. Although the origin of this fact is not fully understood, the observation is supported by dynamical arguments [10] linking the phase transition to chemical freeze-out. The HRG partition function also describes the thermodynamics of a strongly interacting medium in the hadronic phase as obtained in lattice QCD [11,12,13,14,15,16,17].

The proximity of the freeze-out curve to the phase boundary suggests that the QCD phase transition and its related critical properties should be observable in heavy ion collisions. However, an experimental verification of a phase change in a medium created in such collisions requires sensitive probes. In this context, a particular role is attributed to fluctuations of conserved charges [11,18,19,20,21,22,23,24,25].

Recently, it was argued that, at high energies, the history of the system, in particular the path through the QCD cross-over transition from the deconfined and chirally symmetric phase to the hadronic one, may be reflected in fluctuations of conserved charges, specifically in their higher cumulants [23,24,25,26]. The characteristic signature of such transition may thus be manifested in deviations of higher cumulants of the charge distributions from the HRG results, if the freeze-out happens near or at the QCD phase boundary. At vanishing chemical potential, the sixth and higher order cumulants can be negative, also in the hadronic phase, in contrast to predictions from HRG model, where only positive yields are obtained [23]. It is therefore useful to consider the HRG model results on moments of charge fluctuations as a theoretical baseline; any deviation from this could be an indication for critical phenomena at the time of hadronization [11,23,24].

First data on cumulants of the net proton multiplicity were recently obtained by the STAR Collaboration in Au-Au collisions at several energies and centralities [27,28]. The basic properties of the measured fluctuations, in particular of their ratios, are consistent with HRG model expectations [23,28].

In practice, the cumulants of the net proton fluctuations are obtained from the

corresponding probability distribution [31,32,33,34]. As recently noted [35], a direct comparison of the net proton multiplicity distribution, measured in heavy ion collisions, with that of the hadron resonance gas may provide a deeper insight into the relation between chemical freeze-out and the QCD cross-over transition. The comparison is facilitated by the direct link between the net proton probability distribution and the mean number of protons and antiprotons in the HRG model [35]. This eliminates uncertainties connected with the extraction of freeze-out conditions and thus provides a less ambiguous method for confronting the model results with data.

A freeze-out close to the phase boundary should be reflected in a modification of the width and shape of the net proton probability distribution [35]. In the crossover regime from hadronic matter to the quark gluon plasma the width of the distribution is expected to be reduced, compared to the HRG model predictions. If, on the other hand, freeze-out occurs near the chiral critical end point, the width could be enhanced relative to that obtained in the hadron resonance gas. The first STAR results for the net proton probability distribution from Au-Au collision at  $\sqrt{s_{NN}} = 200$  GeV suggest that the width of the experimental distribution may indeed be reduced [35]. In order to scrutinize this effect, a detailed analysis of data on the net-proton probability distributions at different beam energies is necessary.

In this paper we extend our previous results [35] and examine further the significance of the net charge probability distributions as a tool for exploring critical phenomena in heavy ion experiments. In particular, we consider the probability distributions related to the fluctuations of strangeness and electric charge. We show that, in the hadron resonance gas, these distributions, as well as all corresponding cumulants, can be directly linked to mean particle multiplicities. The influence of multi-charged hadrons and quantum statistics on the shape of net charge distributions is discussed. We compute the net proton distribution along the freeze-out line and study its systematics.

In the next section we derive probability distributions of conserved charges in a thermodynamic system and apply the results to the hadron resonance gas. In Section III we discuss the properties of these distributions in the HRG model and make predictions for the net proton probability distribution and the corresponding fluctuations in heavy ion collisions at RHIC energies and at the LHC. Finally, in Section IV we give our conclusions.

## 2 Probability distribution of conserved charges

### 2.1 General case

In statistical physics the probability distribution  $P(N)$  can be obtained directly from the relation between the canonical  $Z(N, T, V)$  and grand canonical  $\mathcal{Z}(\mu_q, T, V)$  partition functions. The thermodynamics of a system with fixed net charge  $N$  is described by  $Z(N, T, V)$ , which is obtained from the density operator

$$Z(N, T, V) = \text{Tr}_N e^{-\beta H}. \quad (1)$$

Here the trace is constrained to configurations with a given net charge  $N$ . The grand canonical partition function

$$\mathcal{Z}(\mu_q, T, V) = \text{Tr} e^{-\beta H + \hat{\mu} N}, \quad (2)$$

where  $\hat{\mu} = \mu_q/T$ , is related to  $Z(N, T, V)$  by the cluster decomposition

$$\mathcal{Z}(\mu_q, T, V) = \sum_N Z(N, T, V) e^{\hat{\mu} N}. \quad (3)$$

The physical meaning of each term in the above sum is the probability of finding a configuration with net charge  $N$ . With the proper normalization, the probability is [1,31,32]

$$P(N) = \frac{1}{\mathcal{Z}(\mu_q, T, V)} Z(N, T, V) e^{\hat{\mu} N}. \quad (4)$$

By eliminating  $\mathcal{Z}(\mu_q, T, V)$  in favor of the thermodynamic pressure  $\ln \mathcal{Z} = VT^3 \hat{p}(T, \hat{\mu})$ , one arrives at the probability distribution

$$P(N) = Z(N, T, V) e^{\hat{\mu} N - VT^3 \hat{p}(T, \hat{\mu})} \quad (5)$$

for finding a state with net charge  $N$  in a system of volume  $V$  at the temperature  $T$ .

The canonical partition function can be directly obtained from the grand canonical one computed at imaginary chemical potential [1],

$$Z(N, T, V) = \frac{1}{2\pi} \int_0^{2\pi} d\theta e^{-i\theta N} \mathcal{Z}(iT\theta, T, V), \quad (6)$$

where the chemical potential was Wick rotated by the substitution  $\hat{\mu} \rightarrow i\theta$ . Equations (4) and (6) define the probability distribution of net charge in a thermal system of volume  $V$ .

The  $n$ -th order cumulant  $\chi_n$  of the net charge  $N$  is obtained by computing the corresponding moments of  $P(N)$ . Alternatively, the cumulants are given

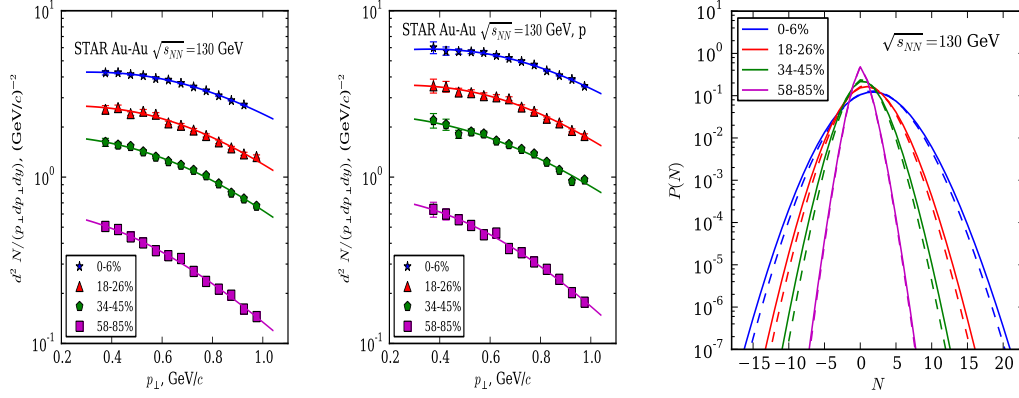


Fig. 1. Left-hand and middle figures: The  $p_t$ -distributions of antiprotons and protons in Au-Au collisions at  $\sqrt{s_{NN}} = 130$  GeV for different centralities [36]. The lines are blast-wave fits [37] to the data. Right-hand figure: The net-proton distribution in the hadron resonance gas computed from Eq. (18) for different centralities. The full lines are obtained using experimental inputs for the proton  $\bar{N}_p$  and antiproton  $\bar{N}_{\bar{p}}$  yields, while the broken-lines are obtained with  $\bar{N}_p$  and  $\bar{N}_{\bar{p}}$  computed in the thermal model with parameters describing the chemical freeze-out [36].

by the generalized susceptibilities

$$\chi_n = \frac{\partial^n \hat{p}(T, \hat{\mu})}{\partial \hat{\mu}^n}. \quad (7)$$

Thus, we have for the susceptibility or the second order cumulant,

$$\chi_2 = \frac{1}{VT^3} (\langle N^2 \rangle - \langle N \rangle^2) = \frac{\partial^2 \hat{p}(T, \hat{\mu})}{\partial \hat{\mu}^2}, \quad (8)$$

where the moments of  $P(N)$  are defined by

$$\langle N^n \rangle = \sum_N N^n P(N). \quad (9)$$

## 2.2 The net-charge distribution in a hadron resonance gas

In a strongly interacting medium there are conservation laws related to the global symmetries of the QCD Lagrangian. In the following, we explore probability distributions of such conserved charges and the corresponding fluctuations. We focus mainly on fluctuations of the net baryon number in hot and dense hadronic matter, but give results also for fluctuations of strangeness and electric charge.

We use the hadron resonance gas partition function to model the thermodynamics of strongly interacting matter. This model yields a good approximation

to the lattice QCD equation of state below the QCD phase transition. In the HRG model the thermodynamic pressure is a sum of meson and baryon contributions. The conservation of baryon number, strangeness and electric charge is accounted for by introducing the corresponding chemical potentials.

In Boltzmann approximation, we can write the thermodynamic pressure in the following form:

$$\beta V p(T, \hat{\mu}) = \sum_{n=0}^{|q|} [z_n e^{n\hat{\mu}} + \bar{z}_n e^{-n\hat{\mu}}]. \quad (10)$$

Here one of the conservation laws is explicitly exhibited. We denote the corresponding chemical potential generically by  $\hat{\mu}$ . Depending on which conservation law is picked, baryon number, electric charge and strangeness, the maximum charge  $q$  take the values  $|q| = 1, 2$  or  $3$ , respectively. The remaining conservation laws are implicitly included in the parameters  $z_n$  and  $\bar{z}_n$ , which encode the thermal phase-space of all particles and antiparticles carrying charge  $n$  and  $-n$ , respectively. Within the HRG model, we find

$$z_n = \sum_{i \in \text{hadrons}} z_n^i, \quad z_n^i = \frac{VT}{2\pi^2} g_i m_i^2 K_2(m_i/T) e^{\beta \vec{l}_i \cdot \vec{\mu}_q}, \quad (11)$$

where the sum is taken over all stable hadrons as well as all hadron resonances. Moreover, the vector  $\vec{l}_i$  represents those charges carried by particle  $i$  that are not explicitly shown in Eq. (10), while  $\vec{\mu}_q$  subsumes the corresponding chemical potentials. The  $\bar{z}_n$  is obtained from Eq. (11) by the replacement  $\vec{\mu} \rightarrow -\vec{\mu}$ .

The phase-space parameters  $z_n$  and  $\bar{z}_n$  are related to the mean-number of particles  $\bar{N}_n$  and antiparticles  $\bar{N}_{-n}$  carrying charge  $n$  and  $-n$ , respectively,

$$\bar{N}_n = z_n \exp(n\hat{\mu}), \quad \bar{N}_{-n} = \bar{z}_n \exp(-n\hat{\mu}). \quad (12)$$

The partition function, where one conservation law is treated exactly, is obtained using Eqs. (6) and (10). We denote the resulting partition function by  $Z^{(|q|)}$ , where  $|q|$  is the relevant maximal charge. We start with the most complex case, i.e. with  $|q| = 3$ . Within the HRG model the corresponding canonical partition function is given by [1]

$$Z^{(3)}(N, T, V) = \sum_{i=-\infty}^{\infty} \sum_{k=-\infty}^{\infty} a_1^{-2i-3k+N} a_2^i a_3^k I_{N-2i-3k}(x_1) I_i(x_2) I_k(x_3), \quad (13)$$

where  $I_N(x)$  is the modified Bessel function. In Eq. (13), we have also introduced the notation

$$a_n = \sqrt{\frac{z_n}{\bar{z}_n}}, \quad \text{and} \quad x_n = 2\sqrt{z_n \bar{z}_n} = 2\sqrt{\bar{N}_n \bar{N}_{-n}} \quad (14)$$

with  $n \in (1, 2, 3)$ . Within the hadron resonance gas model the canonical partition function  $Z^{(3)}$  is appropriate for describing a system with exact conservation of strangeness.

For the electric charge, the appropriate canonical partition function is  $Z^{(2)}$ , since there are single- and double-charged hadrons. We stress, however, that this is correct only within the Boltzmann approximation we consider here. In the electric charge sector this approximation is not suitable, as we will discuss later. The generic form of  $Z^{(2)}$  is obtained from Eq. (13) by taking the limit,  $x_3 \rightarrow 0$  and  $a_3 \rightarrow 1$ . This yields a non-zero contribution only for  $k = 0$ , with  $\lim_{x_3 \rightarrow 0} I_{k=0}(x_3) = 1$ , leaving the summation over  $i$ . The canonical partition function for baryon number conservation,  $Z^{(1)}$ , is then obtained from  $Z^{(2)}$  by taking the corresponding limit,  $x_2 \rightarrow 0$  and  $a_2 \rightarrow 1$ . Again, only the  $i = 0$  contribution survives, leaving an expression in closed form [31]

$$Z^{(1)}(N, T, V) = \left(\frac{z_n}{\bar{z}_n}\right)^{N/2} I_N(2\sqrt{z_n \bar{z}_n}). \quad (15)$$

In the HRG model, the probability  $P(N)$  to find a state with net-charge  $N$  is obtained from Eqs.(4), (10) and (13). We compute explicitly the probability distributions relevant for the phenomenology of heavy-ion collisions, i.e. for strangeness ( $S$ ), electric charge ( $Q$ ) and baryon number ( $B$ ).

Since there are hadrons with strangeness one, two and three, the relevant probability distribution is that obtained from  $Z^{(3)}$ :

$$P(S) = \left(\frac{\bar{S}_1}{\bar{S}_{-1}}\right)^{\frac{S}{2}} \exp \left[ \sum_{n=1}^3 (\bar{S}_n + \bar{S}_{-n}) \right] \sum_{i=-\infty}^{\infty} \sum_{k=-\infty}^{\infty} \left(\frac{\bar{S}_3}{\bar{S}_{-3}}\right)^{k/2} I_k \left(2\sqrt{\bar{S}_3 \bar{S}_{-3}}\right) \\ \left(\frac{\bar{S}_2}{\bar{S}_{-2}}\right)^{i/2} I_i \left(2\sqrt{\bar{S}_2 \bar{S}_{-2}}\right) \left(\frac{\bar{S}_1}{\bar{S}_{-1}}\right)^{-i-3k/2} I_{2i+3k-S} \left(2\sqrt{\bar{S}_1 \bar{S}_{-1}}\right), \quad (16)$$

where  $\bar{S}_s$  and  $\bar{S}_{-s}$  denote the mean-number of particles and antiparticles carrying strangeness  $s$ , where  $s \in (1, 2, 3)$  (see Eq. (12)).

For the electric charge, treated in Boltzmann approximation, the corresponding probability is given by

$$P(Q) = \left(\frac{\bar{Q}_1}{\bar{Q}_{-1}}\right)^{\frac{Q}{2}} \exp \left[ \sum_{n=1}^2 (\bar{Q}_n + \bar{Q}_{-n}) \right] \sum_{i=-\infty}^{\infty} \left(\frac{\bar{Q}_2}{\bar{Q}_{-2}}\right)^{i/2} I_i \left( 2\sqrt{\bar{Q}_2 \bar{Q}_{-2}} \right) \\ \left(\frac{\bar{Q}_1}{\bar{Q}_{-1}}\right)^{-i} I_{2i-Q} \left( 2\sqrt{\bar{Q}_1 \bar{Q}_{-1}} \right), \quad (17)$$

where  $\bar{Q}_q$  and  $\bar{Q}_{-q}$  denote the mean number of particles and antiparticles with electric charge  $q$  and  $-q$  respectively, with  $q \in (1, 2)$ .

Finally, the probability  $P(B)$  of net-baryon number  $B$  can be expressed in terms of the mean-number of baryons  $\bar{B}_1$  and antibaryons  $\bar{B}_{-1}$  [35] by the Skellam distribution,

$$P(B) = \left(\frac{\bar{B}_1}{\bar{B}_{-1}}\right)^{\frac{B}{2}} I_B \left( 2\sqrt{\bar{B}_1 \bar{B}_{-1}} \right) \exp \left[ \bar{B}_1 + \bar{B}_{-1} \right]. \quad (18)$$

Equations (16)–(18) determine the probability distributions for the fluctuations of net strangeness, electric charge and baryon number in a hadron resonance gas in equilibrium and under Boltzmann statistics. We note that the probability distributions of the HRG depend only on the mean-number of charged particles and antiparticles.

### 3 Net-proton distribution in heavy ion collisions

#### 3.1 Probability distributions

The mean number of particles  $\bar{N}_n$  and antiparticles  $\bar{N}_{-n}$  obtained in experiment can, when available, be used directly in Eqs. (16–18), where the volume and all thermal parameters have been eliminated. Thus, predictions of the HRG model can be compared with data in an unambiguous way, avoiding further model assumptions. In particular, using measured multiplicities  $\bar{N}_n$  and  $\bar{N}_{-n}$  has the advantage that experimental cuts are included consistently for all quantities. We note that for a comparison of data to theory the experimental results have to be corrected for effects due to overall baryon, strangeness, and charge conservation.

Alternatively, in the HRG model the mean number of particles  $\bar{N}_n$  and antiparticles  $\bar{N}_{-n}$  entering  $P(N)$  in Eqs. (16–18) can, given the thermal and volume parameters, be computed using Eq. (12). In applications of the HRG model to



heavy-ion phenomenology the thermal parameters are determined along the chemical freeze-out curve. The volume can then be fixed to reproduce the net charge number or particular particle yields.

At present, the first approach can be applied only for the net baryon multiplicity distribution. The electric charge and strangeness probability distributions require experimental input on yields of all charge states in the acceptance window where the probability distributions are obtained. At present, such data are not available for strangeness and electric charge. On the other hand, first data on charge fluctuations and higher order cumulants of net proton multiplicities were recently obtained by the STAR Collaboration in Au-Au collisions at several collision energies [27,28]. The data were taken at mid-rapidity in a restricted range of transverse momenta,  $0.4 \text{ GeV} \leq p_T \leq 0.8 \text{ GeV}$ .

Consequently, in the following, we focus on the net-proton probability distributions in the hadron resonance gas model.

The probability distribution, Eq. (18), is readily generalized to protons in a momentum window. Due to the factorization of the grand canonical single-particle partition function in momentum space, Eq. (3) yields a normalized probability distribution, when both partition functions are restricted to the same momentum window. Similarly, the limitation to protons follows from the factorization of the contribution of any particle species to  $\mathcal{Z}$ . Consequently, in the HRG model the probability distribution of net proton number in a momentum window,  $\delta N_p = \bar{N}_p - \bar{N}_{\bar{p}}$ , is obtained from Eq. (18) by simply replacing the mean number of baryons  $\bar{B}_1$  and anti-baryons  $\bar{B}_{-1}$  by that of protons  $\bar{N}_p$  and antiprotons  $\bar{N}_{\bar{p}}$  in the same kinematic window.

Thus, we can compute the net-proton distribution using Eq. (18), provided we have access to the mean values  $\bar{N}_p$  and  $\bar{N}_{\bar{p}}$  measured in the same kinematic window. Recently, such studies were performed in Ref. [35], using the STAR data [27,36] on  $p_t$ -distributions of antiprotons, the mean number of net protons as well as  $P(N)$  for Au-Au collisions at  $\sqrt{s_{NN}} = 200 \text{ GeV}$  and at several centralities. To assess the dependence of  $P(N)$  in A-A collisions on beam energy, we extend these studies to different energies along the chemical freeze-out curve.

Unambiguous predictions of the model for the net proton probability distribution can be obtained in Au-Au collisions at  $\sqrt{s_{NN}} = 130 \text{ GeV}$  as well as in Pb-Pb collisions at the LHC, since at these energies the  $p_t$ -distributions of protons and antiprotons are available [36,38].

In Fig. 1 we show the  $p_t$ -spectra of protons and antiprotons at  $\sqrt{s_{NN}} = 130 \text{ GeV}$  obtained by the STAR Collaboration [36]. By fitting these spectra with the blast-wave model [37] and integrating the data in the range  $0.4 \text{ GeV} \leq p_t \leq 0.8 \text{ GeV}$ , we find  $\bar{N}_p$  and  $\bar{N}_{\bar{p}}$  for the different centralities.

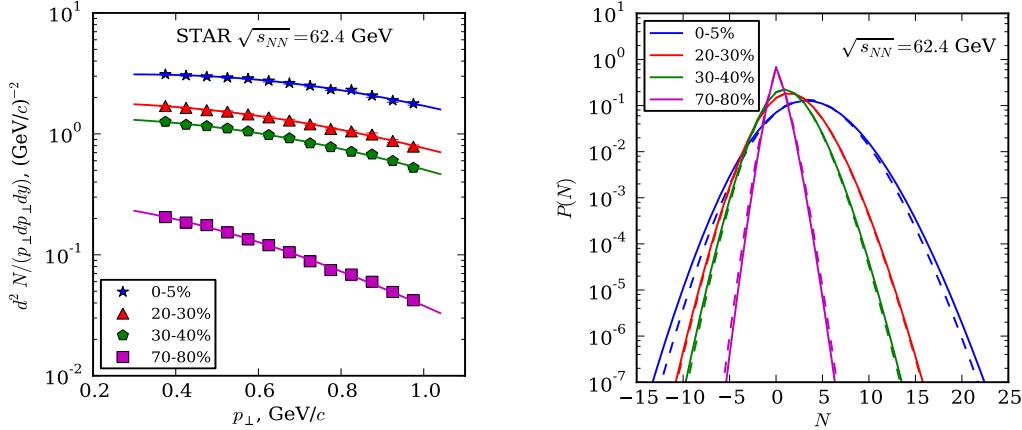


Fig. 2. Left-hand figure: The  $p_t$ -distribution of antiprotons obtained by the STAR Collaboration in Au-Au collisions at  $\sqrt{s_{NN}} = 62.4$  GeV for different centralities [36]. The lines are blast-wave fits [37] to the data. Right-hand figure: The net-proton distribution calculated in the hadron resonance gas from Eq. (18) for Au-Au collisions at  $\sqrt{s_{NN}} = 62.4$  GeV at different centralities. The full-lines are obtained with experimental inputs for the proton  $\bar{N}_p$  yields and the mean net baryon number  $M = \bar{N}_p - \bar{N}_{\bar{p}}$ , while the broken-lines are obtained with  $\bar{N}_p$  and  $\bar{N}_{\bar{p}}$  calculated in the thermal model with parameters describing the chemical freeze-out [36].

In the right panel of Fig. 1 we show the corresponding HRG result for the net proton multiplicity distribution in Au+Au collisions at  $\sqrt{s_{NN}} = 130$ . Also shown in this figure are the results for  $P(N)$  obtained within the HRG model with  $\bar{N}_p$  and  $\bar{N}_{\bar{p}}$  computed at the chemical freeze-out using the thermal parameters of Ref. [36]. The volume was fixed by requiring that the measured mean-number of protons be reproduced. The overall agreement of the two methods is satisfactory. Nevertheless, a direct calculation of  $P(N)$  from the measured yields of protons and antiprotons is preferable, since it is unaffected by systematic errors in the thermal parameters.

In order to find  $P(N)$  in Au-Au collisions at  $\sqrt{s_{NN}} = 62.4$  GeV, we used the measured  $p_t$ -spectra of antiprotons [36] to determine the antiproton multiplicity. The proton yield was then fixed using the measured mean net proton number [27,28]. We stress that the data on net-proton number are not corrected for efficiency [27,29]. This implies a systematic uncertainty in our results. The resulting distributions for different centralities are shown in Fig. 2. Again, we also show results of the thermal model, where  $\bar{N}_p$  and  $\bar{N}_{\bar{p}}$  are computed at the chemical freeze-out using the thermal parameters of Ref. [36]. The two methods give similar results on  $P(N)$  at all centralities.

Recently, the STAR Collaboration has also presented preliminary data on moments of the net-proton distribution in central Au-Au collisions at  $\sqrt{s_{NN}} = 7.7$ , 11.5 and 39 GeV. However, at these energies the corresponding  $p_t$ -spectra of protons and antiprotons are not available. Thus, for these energies we com-

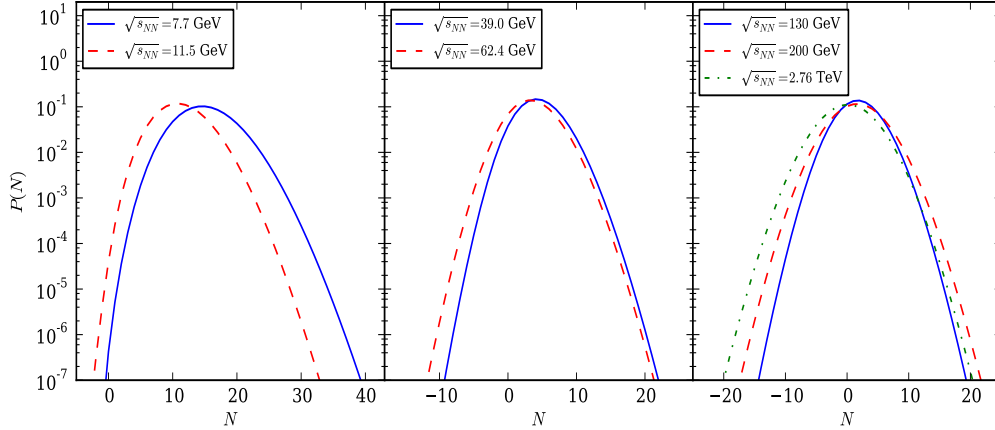


Fig. 3. Predictions of the hadron resonance gas model for the net proton probability distribution in central nucleus-nucleus collisions at different energies. The results for Au-Au collisions at  $\sqrt{s_{NN}} = 62.4$  and  $\sqrt{s_{NN}} = 130$  GeV are obtained using Eq. (18) with experimental inputs for the proton  $\bar{N}_p$  and antiproton  $\bar{N}_{\bar{p}}$  yields extracted from the  $p_t$  spectra of the STAR Collaboration [36]. The probability distribution for Pb-Pb collisions at  $\sqrt{s_{NN}} = 2.74$  TeV is obtained using Eq. (18) with experimental inputs for  $\bar{N}_p$  and  $\bar{N}_{\bar{p}}$  extracted from the preliminary  $p_t$ -spectra of the ALICE Collaboration [38]. At lower energies,  $P(N)$  is computed with  $\bar{N}_p$  and  $\bar{N}_{\bar{p}}$  determined at the chemical freeze-out with thermal parameters from Ref. [2]. The required experimental inputs on mean net-proton numbers are from STAR Collaboration [27,28].

puted  $P(N)$  in the hadron resonance gas using the proton and antiproton yields obtained in the thermal model at chemical freeze-out with the thermal parameters of Ref. [2]. The volume was fixed by fitting the mean number of net protons to the STAR data [30]. The resulting probability distributions  $P(N)$  for these three energies are shown in Fig. 3.

In order to assess the possible role of dynamical effects on the probability distribution, we compare in Fig. 4 the STAR data on  $P(N)$  in Au-Au collisions at  $\sqrt{s_{NN}} = 200$  GeV and the HRG results of Ref. [35] with the net proton probability distribution obtained with the UrQMD event generator. Deviations of the thermal model from the data and their possible origin were discussed in Ref. [35]. We note that the distribution obtained in the UrQMD model is much narrower than the data. The reason for this remains to be clarified.

In Fig. 3 we summarize the HRG model results for the net proton distributions in central nucleus-nucleus at energies spanning from  $\sqrt{s_{NN}} = 7.7$  GeV up to  $\sqrt{s_{NN}} = 2.74$  TeV. The probability distribution at the LHC energy is computed with proton and antiproton yields obtained by integrating the preliminary data on  $p_t$ -spectra of the ALICE Collaboration [38] in the  $p_t$  range ( $0.4 \text{ GeV} < p_t < 0.8 \text{ GeV}$ ). The  $P(N)$  distributions shown in Figs (1-3) can be compared directly to properly normalized data from RHIC and LHC.

### 3.2 Beam energy systematics of $P(N)$ and its cumulants in heavy ion collisions

As seen in Fig. 3, there are systematic changes in the net-proton probability distributions in central heavy ion collisions with increasing beam energy. There is a clear asymmetry in  $P(N)$  at lower energies, which is largely eliminated at the LHC. With increasing  $\sqrt{s_{NN}}$ , there is a corresponding shift of the maximum of  $P(N)$  from a nonzero value of  $N$  towards  $N = 0$ . These properties of  $P(N)$  are direct consequences of the decreasing net baryon density with increasing beam energy.

A rather striking feature, seen in Fig. 3, is that in the entire energy range from the lowest RHIC energies up to LHC energies the maximum of  $P(N)$ , is almost independent of energy. This is unexpected, as it is well known that in heavy ion collisions the total *density* of baryons plus antibaryons in the whole  $p_t$ -range at mid-rapidity is approximately constant along the chemical freeze-out curve [39]. The yield of both protons and anti-protons thus changes considerably with energy. On the other hand, as we show in the following, the maximum of  $P(N)$  is proportional to  $[\bar{N}_p + \bar{N}_{\bar{p}}]^{-1/2}$ .

The maximum value of  $P(N)$  can be obtained analytically from Eq. (18) in two limiting cases: for very high and very low energies. The probability  $P(N)$  has its maximum at some value of  $N \approx [\langle N \rangle]$ , where  $[N]$  denotes an integer part of  $N$ .

At high energy, the mean net-proton number is small,  $\langle N \rangle = 0$ , while  $\bar{N}_p$  is large. Therefore, the maximum of  $P(N)$  appears at  $N \approx [\langle N \rangle] = 0$  and

$$P_{max}^{\sqrt{s} \rightarrow \infty} \simeq I_0 \left( 2\sqrt{\bar{N}_p \bar{N}_{\bar{p}}} \right) e^{-(\bar{N}_p + \bar{N}_{\bar{p}})} \approx \left[ 2\pi(\bar{N}_p + \bar{N}_{\bar{p}}) \right]^{-1/2}, \quad (19)$$

where we used the asymptotic expansion of the Bessel function [40],

$$I_\nu(x \gg \nu + 1) \approx \frac{e^x}{\sqrt{2\pi x}}, \quad (20)$$

as well as that  $\bar{N}_p \approx \bar{N}_{\bar{p}}$  and  $2[\bar{N}_p \cdot \bar{N}_{\bar{p}}]^{1/2} \approx (\bar{N}_p + \bar{N}_{\bar{p}})$ .

At low energies, on the other hand, the number of antiprotons is very small  $\bar{N}_{\bar{p}} \ll \bar{N}_p$ . Consequently, the argument of the Bessel function in Eq. (18) is much less than its order. Then [40]

$$I_\nu(x) \approx \frac{(x/2)^\nu}{\Gamma(\nu + 1)} \approx \frac{(x/2)^\nu e^\nu}{\sqrt{2\pi\nu\nu^\nu}}, \quad (21)$$

and the maximum probability at low energy is obtained from

$$P_{max}^{\sqrt{s} \rightarrow 0} \approx \frac{(\bar{N}_p \bar{N}_{\bar{p}})^{\bar{N}_p/2} e^{\bar{N}_p} \left( \frac{\bar{N}_p}{\bar{N}_{\bar{p}}} \right)^{\bar{N}_p/2}}{\left[ 2\pi \bar{N}_p \right]^{1/2} \bar{N}_p^{\bar{N}_p}} e^{-\bar{N}_p} \approx \left[ 2\pi(\bar{N}_p + \bar{N}_{\bar{p}}) \right]^{-1/2}, \quad (22)$$

where we use  $\bar{N}_p \pm \bar{N}_{\bar{p}} \approx \bar{N}_p$ .

Thus, at high as well as at low energies, the maximal value of the net proton probability distribution

$$P_{max} \approx \frac{1}{\left[ 2\pi(\bar{N}_p + \bar{N}_{\bar{p}}) \right]^{1/2}} \quad (23)$$

is approximately equal and determined by the total mean number of protons and antiprotons.

At intermediate energies, none of the approximations used above hold. However, near the maximum, we can approximate  $P(N)$  by a Gaussian,

$$P(N) \approx \frac{1}{\sqrt{2\pi\sigma^2}} e^{-\frac{(N-\bar{N})^2}{2\sigma^2}}, \quad (24)$$

with the maximum value

$$P_{max} = \frac{1}{\sqrt{2\pi\sigma^2}}. \quad (25)$$

In the hadron resonance gas, the variance is directly related to the total number of protons and antiprotons

$$\sigma^2 = \bar{N}_p + \bar{N}_{\bar{p}}. \quad (26)$$

Consequently, we conclude that the maximum value of the net proton probability distribution is, to a good approximation, determined by

$$P_{max}^{HRG} \approx \frac{1}{\left[ 2\pi(\bar{N}_p + \bar{N}_{\bar{p}}) \right]^{1/2}} \quad (27)$$

irrespective of the collision energy. On the other hand, as  $P_{max}^{HRG}$  depends only weakly on the beam energy (see Fig. 3), the value of  $\bar{N}_p + \bar{N}_{\bar{p}}$  in the acceptance window has to be essentially energy independent.

In Fig. 5-right we show the energy dependence of the variance  $\sigma = \left[ \bar{N}_p + \bar{N}_{\bar{p}} \right]^{1/2}$  in heavy ion collisions obtained at mid rapidity with  $|y| < 0.5$ , in the transverse momentum window,  $0.4 \text{ GeV} < p_t < 0.8 \text{ GeV}$ . The small variation of  $\sigma$ , seen in this figure, is consistent with the observed weak dependence of the maximum of  $P(N)$  on  $\sqrt{s_{NN}}$ , which thus seems to be a consequence of the

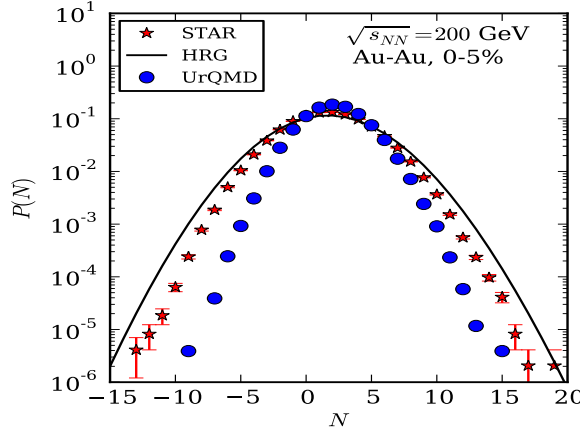


Fig. 4. The net-proton probability distribution in central Au-Au collisions at  $\sqrt{s_{NN}} = 200\text{ GeV}$ . The HRG results are from Ref. [35], while the data are due to the STAR Collaboration [27]. Also shown are results obtained with the UrQMD event generator [41] from a sample of  $10^5$  events.

particular  $p_t$ -cut applied to the transverse-momentum distributions of protons and antiprotons.

In the hadron resonance gas, not only the variance, but also all higher moments of the net proton distribution can be expressed in terms of the mean number of protons and antiprotons. Indeed, using Eqs. (7) and (10), one finds for  $n = 1$ ,

$$\chi_{2n} = \frac{1}{VT^3} (\bar{N}_p + \bar{N}_{\bar{p}}), \quad \chi_{2n+1} = \frac{1}{VT^3} (\bar{N}_p - \bar{N}_{\bar{p}}). \quad (28)$$

Consequently, the skewness  $S = VT^3\chi_3/(VT^3\chi_2)^{3/2}$  and the kurtosis  $\kappa = VT^3\chi_4/(VT^3\chi_2)^2$  are directly related to  $\bar{N}_p$  and  $\bar{N}_{\bar{p}}$  by

$$S = \frac{\bar{N}_p - \bar{N}_{\bar{p}}}{(\bar{N}_p + \bar{N}_{\bar{p}})^{3/2}}, \quad \kappa = \frac{1}{\bar{N}_p + \bar{N}_{\bar{p}}}. \quad (29)$$

The energy dependence of skewness and kurtosis is shown in Fig. 5-right. The weak energy dependence of  $(\bar{N}_p + \bar{N}_{\bar{p}})$  implies that the kurtosis and all even cumulants are essentially independent of beam energy. By contrast, the skewness and all odd cumulants are strongly decreasing functions of energy, and approach zero at high energies, where  $N_{\bar{p}} \simeq N_p$ .

We have seen that in the HRG model all moments of net proton distribution can be expressed directly in terms of the mean-number of protons and antiprotons. This can be generalized to moments of the fluctuations of strangeness

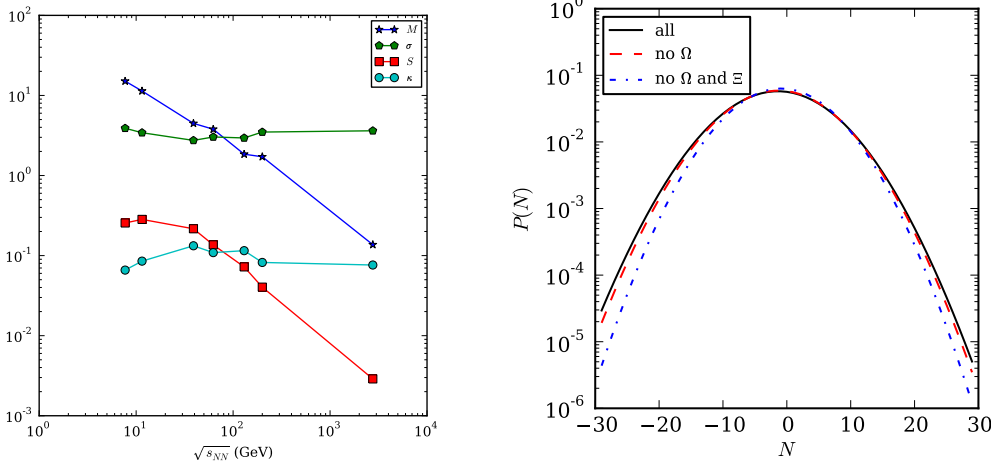


Fig. 5. Left-hand figure: The mean (M), variance ( $\sigma$ ), skewness (S) and kurtosis ( $\kappa$ ) for net proton number in central Au-Au collisions computed using the probability distributions shown in Fig. 3. Right-hand figure: The probability distribution for net-strangeness in a gas composed of ( $K^+$ ,  $\Lambda$ ,  $\Xi$ ,  $\Omega$ ) and their antiparticles at  $T \simeq m_\pi$ . The distribution is calculated with and without multi-strange baryons.

and electric charge. Indeed, using Eqs. (7) and (10) one finds, that in general

$$\chi_{2k} = \frac{1}{VT^3} \sum_{n=1}^{|q|} (\bar{N}_n + \bar{N}_{\bar{n}}) n^{2k}, \quad \chi_{2k+1} = \frac{1}{VT^3} \sum_{n=1}^{|q|} (\bar{N}_n - \bar{N}_{\bar{n}}) n^{2k+1}. \quad (30)$$

where  $|q| = 1, 2$  or  $3$  for baryon number, electric charge and strangeness, respectively. For the electric charge fluctuations this implies that

$$\chi_1^Q = \frac{\bar{N}_1 - \bar{N}_{-1} + 2(\bar{N}_2 - \bar{N}_{-2})}{VT^3}, \quad \chi_2^Q = \frac{\bar{N}_1 + \bar{N}_{-1} + 4(\bar{N}_2 + \bar{N}_{-2})}{VT^3} \quad (31)$$

$$\chi_3^Q = \frac{\bar{N}_1 - \bar{N}_{-1} + 8(\bar{N}_2 - \bar{N}_{-2})}{VT^3}, \quad \chi_4^Q = \frac{\bar{N}_1 + \bar{N}_{-1} + 16(\bar{N}_2 + \bar{N}_{-2})}{VT^3}, \quad (32)$$

where  $\bar{N}_1$  ( $\bar{N}_{-1}$ ) and  $\bar{N}_2$  ( $\bar{N}_{-2}$ ) are the mean numbers of particles with charge  $+1$  ( $-1$ ) and  $+2$  ( $-2$ ) respectively. Thus, in the HRG model, the experimental input on the mean number of charged and multi-charged particles is sufficient to compute the net charge probability distribution and the corresponding moments. We stress, however, that this is only the case in the Boltzmann approximation, which in the case of electric charge is a poor approximation.

#### 4 The influence of multi-charged particles and quantum statistics on $P(N)$

The influence of multi-charged particles on fluctuations was discussed in Ref. [11]. In the HRG model, the product of kurtosis and variance of the net baryon number,  $\kappa\sigma^2$ , which receives contributions from singly charged particles only, is always equal to unity. This result does not depend on the hadron mass spectrum nor on the thermal parameters. However, for fluctuations of the electric charge, the contribution of particles with charge two,  $\Delta^{++}$  and  $\bar{\Delta}^{--}$ , leads to a non-trivial  $T$  and  $\mu$  dependence of this quantity [11]. Furthermore, a straightforward calculation shows that in an ideal pion gas,  $\kappa\sigma^2$  is temperature dependent and differs from unity, due to quantum statistics effects.

Clearly these effects should be reflected in the corresponding probability distribution. To illustrate the influence of multi-charged particles and of quantum statistics we consider two simple models: *i*) a gas composed of  $\Lambda$ ,  $\Xi$  and  $\Omega$  and their antiparticles and *ii*) an ideal pion gas. Within the first model we compute  $P(S)$  and within the second  $P(Q)$ . In Figs. 5-right and 6-right we show the probability distributions of the net strangeness and net electric charge calculated in the models defined above.

To assess the influence of multi-charged particles, we compare the results with  $P(N)$  computed using Eq. (18), which accounts only for singly charged particles. Since the multi-charged particles are heavy, their contribution to the mean-charge is negligible. Consequently, the position of the maximum of  $P(S)$  is not changed when these states are included. However, the contribution of double- and triple-charged particles modifies the tail of the probability distribution considerably, and therefore also the higher order moments. Thus, a comparison of fluctuations in the hadron resonance gas model with data, must account for multi-charged particles, since they are included in the data through their decay products.

The probability distributions in Eqs. (16–18) are valid only in Boltzmann approximation. This approximation is justified for the net strange and net baryon number probability distributions. However, owing to the small mass of the pion, quantum statistics must be included in studies of charge fluctuations. The effect of the corrections to the Boltzmann approximation due to quantum statistics is similar to that induced by multi-charged states, and could affect the net charge distribution  $P(Q)$ .

Indeed, the pressure of charged pions at temperature  $T$  and electric charge chemical potential  $\mu$  can be expanded in powers of the fugacity,  $e^{\pm\mu/T}$ ,

$$\frac{p_{\pi^+} + p_{\pi^-}}{T^4} = \frac{1}{\pi^2} \sum_{l=1}^{\infty} d_l (\beta m_l)^2 K_2(\beta m_l) \cosh(q_l \beta \mu), \quad (33)$$



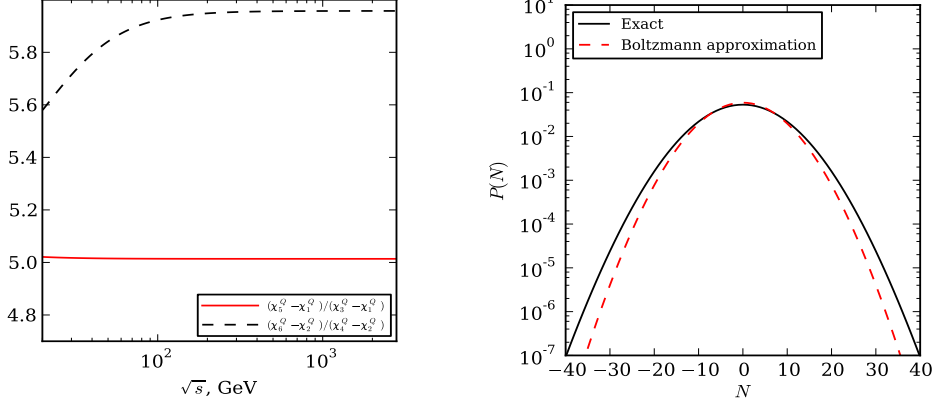


Fig. 6. Left-hand figure: The ratios  $R_5$  and  $R_6$  from Eq. (37) in the HRG model along the freeze-out line. Right-hand figure: The probability distributions for net-electric charge in a pion gas at  $T \simeq m_\pi$  calculated with quantum statistics (Exact) and in the Boltzmann approximation.

where  $m_l = l m_\pi$ ,  $d_l = 1/l^4$  and  $q_l = l$ . Thus, the pion pressure, Eq. (33), can be viewed as a sum of Boltzmann contributions owing to particles with charge  $q_l$  mass  $m_l$  and degeneracy factor  $d_l$ .

At  $\mu = 0$ , the pion contribution to the  $n$ -th order cumulant of the electric charge reads

$$\chi_n^Q = \frac{m^2}{\pi^2 T^2} \sum_{l=1}^{\infty} l^{n-2} K_2(l\beta m_\pi). \quad (34)$$

An approximation to  $\chi_n^Q$  is obtained by truncating the series (34) at some order  $l = l^*$ . The value of  $l^*$ , which yields a good approximation to the exact result, depends strongly on the order of the cumulant.

At temperatures  $T \simeq m_\pi$  the dominant contribution to the cumulants  $\chi_n^Q$  with  $n \leq 5$  is due to the  $l = 1$  and  $l = 2$  terms. In other words, in the HRG model, the next to leading order Boltzmann approximation is sufficient to quantify cumulants up to fifth order. Consequently, Eqs. (31) and (32) remain valid if the effective charge-2 pion contribution in the expansion (34) is taken into account. However, this is not the case for the sixth- and higher-order cumulants. The dominant contribution to  $\chi_6^Q$  is due to the  $l = 3$  term in Eq. (34). Consequently, Eq. (30) implies that the sixth-order cumulant of the electric charge is well approximated by

$$\chi_6^Q \simeq \frac{1}{VT^3} \left[ \bar{N}_1 + \bar{N}_{\bar{1}} + 2^6(\bar{N}_2 + \bar{N}_{2\pi} + \bar{N}_{\bar{2}} + \bar{N}_{\bar{2}\pi}) + 3^6(\bar{N}_{3\pi} + \bar{N}_{3\bar{\pi}}) \right], \quad (35)$$

where  $N_1$  ( $N_{-1}$ ) and  $N_2$  ( $N_{-2}$ ) are the numbers of particles with charge  $+1$  ( $-1$ ) and  $+2$  ( $-2$ ) respectively, while  $\bar{N}_{k\pi}$  and  $\bar{N}_{k\bar{\pi}}$  are the  $k$ -th order corrections to

the Boltzmann approximation for the charged pions numbers

$$\bar{N}_{k\pi} = \frac{VT^3}{2\pi^2} \left( \frac{m_\pi}{kT} \right)^2 K_2 \left( \frac{km_\pi}{T} \right) e^{k\beta\mu}. \quad (36)$$

The number of antipions,  $\bar{N}_{\bar{k}\pi}$ , is obtained from Eq. (36) by the replacement  $\mu \rightarrow -\mu$ , where  $\mu$  is the electric charge chemical potential.

The influence of quantum statistics on fluctuations of the electric charge can be made more transparent by considering the ratios:

$$R_5^Q = \frac{\chi_5^Q - \chi_1^Q}{\chi_3^Q - \chi_1^Q}, \quad R_6^Q = \frac{\chi_6^Q - \chi_2^Q}{\chi_4^Q - \chi_2^Q}. \quad (37)$$

If *only* doubly charged contributions are included in Eqs. (30–32) and (35), the ratios  $R_5^Q = R_6^Q = 5$  are independent of temperature and chemical potential. Any deviation from this value signal contributions emanating from the third- and higher-order corrections owing to quantum statistics.

In Fig. 6-left, the effect of quantum statistics is illustrated by the ratios  $R_5$  and  $R_6$  obtained in the HRG model along the chemical freeze-out line. As shown, the ratio  $R_5^Q$  is indeed within  $< 1$  % consistent with the result from Eqs. (30–32), while  $R_6^Q$  deviates by up to 20 % due to the missing effective triply charged pionic contribution to  $\chi_6^Q$ .

The effect of quantum statistics is also reflected in the net electric charge probability distribution. In Fig. 6-right we show that the inclusion of quantum statistics results in a broadening of the net charge probability distribution of an ideal pion gas, which is indeed very similar to the effect of multi-charged particles.

In the HRG the probability distribution of the electric charge, due to the relevant contributions from the second and the third order pionic quantum statistics corrections, can be explicitly calculated by applying Eq. (16) instead of Eq. (17).

## 5 Conclusions

We have analyzed the properties of the net charge probability distributions in heavy-ion collisions within the hadron resonance gas model. Within this model, these distributions and the corresponding cumulants are linked directly to other observables, and can be determined from the mean number of charged and multi-charged particles.

Differences between the probability distributions for strangeness, electric charge and net-baryon number were discussed and the role of multi-charged particles and quantum statistics was explored. A comparison of the UrQMD results for the net baryon probability distribution in central Au-Au collisions at  $\sqrt{s_{NN}} = 200$  GeV with data and with the hadron resonance gas model was also presented. We find that the distribution obtained within the UrQMD model is much narrower than both the experimental distribution and that of the hadron resonance gas.

The comparison of model results with data on net proton distributions and the corresponding moments is particularly transparent. This is because, within the hadron resonance gas model, these quantities are determined entirely by the measured yields of protons and antiprotons. This offers an unambiguous route for confronting this particular model with experimental data.

We have presented model predictions for net proton probability distributions  $P(N)$  in heavy ion collisions at RHIC and at LHC energies and computed the centrality dependence of  $P(N)$  in Au-Au collisions at  $\sqrt{s_{NN}} = 62.4$  and 130 GeV. The results for  $P(N)$  obtained in the hadron resonance gas along with the chemical freeze-out curve can be compared with data. Such a comparison would be an important test of the relation between the chemical freeze-out and the QCD cross-over line in heavy ion experiments.

## Acknowledgments

We acknowledge discussions with Alexander Kalweit, Ilya Selyuzhenkov, Johanna Stachel and Nu Xu. Comments from Chen Lizhu are also kindly acknowledged. K.R. acknowledges partial support of the Polish Ministry of National Education (MEN). The work of F.K. and V.S. was supported in part by contract DE-AC02-98CH10886 with the U.S. Department of Energy. B. F. acknowledges partial support by EMMI.

## References

- [1] P. Braun-Munzinger, K. Redlich, J. Stachel, in Quark-Gluon Plasma 3, Eds. R.C. Hwa and X.N. Wang, (World Scientific Publishing, 2004); A. Andronic, P. Braun-Munzinger, J. Stachel, Acta Phys. Polon. B**40**, 1005 (2009).
- [2] J. Cleymans, H. Oeschler, K. Redlich, S. Wheaton, Phys. Rev. C**73**, 034905 (2006).
- [3] M. M. Aggarwal *et al.* [ STAR Collaboration ], Phys. Rev. C**83**, 034910 (2011).

- [4] J. Cleymans, K. Redlich, Phys. Rev. Lett. **81**, 5284 (1998).
- [5] P. Braun-Munzinger, J. Stachel, Nucl. Phys. **606**, 320 (1996).
- [6] Y. Aoki, S. Borsanyi, S. Durr, Z. Fodor, S. D. Katz, S. Krieg, K. K. Szabo, JHEP **0906**, 088 (2009).
- [7] A. Bazavov et. al. (HotQCD collaboration), arXiv:1111.1710 [hep-lat].
- [8] O. Kaczmarek, *et al.*, Phys. Rev. D**83**, 014504 (2011).
- [9] G. Endrodi, et. al., JHEP 1104, 011 (2011).
- [10] P. Braun-Munzinger, J. Stachel, C. Wetterich, Phys. Lett. B**596**, 61 (2004).
- [11] S. Ejiri, F. Karsch, K. Redlich, Phys. Lett. B**633**, 275(2006). F. Karsch, S. Ejiri, K. Redlich, Nucl. Phys. A**774**, 619 (2006).
- [12] F. Karsch, K. Redlich, A. Tawfik, Phys. Lett. B**571**, 67 (2003). Eur. Phys. J. C**29**, 549 (2003).
- [13] K. Redlich, F. Karsch, A. Tawfik, J. Phys. G**30**, S1271 (2004).
- [14] C. R. Allton, M. Doring, S. Ejiri, S. J. Hands, O. Kaczmarek, F. Karsch, E. Laermann, K. Redlich, Phys. Rev. D**71**, 054508 (2005).
- [15] S. Borsanyi et al., [Wuppertal-Budapest Collaboration], Nucl. Phys. A**855**, 253 (2011).
- [16] P. Huovinen, P. Petreczky, Nucl. Phys. A**837**, 26 (2010).
- [17] A. Majumder, B. Muller, Phys. Rev. Lett. **105**, 252002 (2010).
- [18] M. A. Stephanov, K. Rajagopal, E. V. Shuryak, Phys. Rev. Lett. **81**, 4816 (1998)
- [19] Y. Hatta, T. Ikeda, Phys. Rev. D**67**, 014028 (2003).
- [20] S. Jeon, V. Koch, Phys. Rev. Lett. **85**, 2076 (2000). Phys. Rev. Lett. **83**, 5435 (1999).
- [21] M. Asakawa, U. W. Heinz, B. Muller, Phys. Rev. Lett. **85**, 2072 (2000).
- [22] C. Sasaki, B. Friman, K. Redlich, Phys. Rev. Lett. **99**, 232301 (2007). Phys. Rev. D**77**, 034024 (2008).
- [23] F. Karsch, K. Redlich, Phys. Lett. B**695**, 136 (2011).
- [24] B. Friman, F. Karsch, K. Redlich, V. Skokov, Eur. Phys. J. C**71**, 1694 (2011).
- [25] F. Karsch, K. Redlich, Phys. Rev. D**84**, 051504 (2011).
- [26] V. Skokov, B. Friman, K. Redlich, [arXiv:1108.3231 [hep-ph]].
- [27] M. M. Aggarwal *et al.* [ STAR Collaboration ], Phys. Rev. Lett. **105**, 022302 (2010).

- [28] X. Luo, B. Mohanty, H. G. Ritter, N. Xu, [arXiv:1105.5049 [nucl-ex]].
- [29] X. Luo, arXiv:1109.0593 [physics.data-an].
- [30] B. Mohanty, for STAR Collaboration, plenary talk at Quark Matter 2011, Annecy, France.
- [31] J. Cleymans, K. Redlich, L. Turko, Phys. Rev. C **71**, 047902 (2005).
- [32] J. Cleymans, P. Koch, Z. Phys. C **52**, 137 (1991). C. M. Ko, V. Koch, Z. Lin, K. Redlich, M. Stephanov, X. N. Wang, Phys. Rev. Lett. **86**, 5438 (2001).
- [33] Z. -W. Lin, C. M. Ko, Phys. Rev. C **64**, 041901 (2001).
- [34] V. V. Begun, M. Gazdzicki, M. I. Gorenstein, M. Hauer, V. P. Konchakovski, B. Lungwitz, Phys. Rev. C **76**, 024902 (2007). V. V. Begun, M. Gazdzicki, M. I. Gorenstein, O. S. Zozulya, Phys. Rev. C **70**, 034901 (2004).
- [35] P. Braun-Munzinger, B. Friman, F. Karsch, K. Redlich, V. Skokov, arXiv:1107.4267.
- [36] B. I. Abelev *et al.* [ STAR Collaboration ], Phys. Rev. C **79**, 034909 (2009).
- [37] E. Schnedermann, J. Sollfrank, U. Heinz, Phys. Rev. C **48**, 2462 (1993).
- [38] M. Floris *et al.*, for ALICE Collaboration, plenary talk at Quark Matter 2011, Annecy, France, arXiv:1108.3257 [hep-ex].
- [39] P. Braun-Munzinger, J. Stachel, J. Phys. G **28**, 1971 (2002).
- [40] M. Abramowitz, I.A. Stegun. "Handbook of Mathematical Function", (Dover Publications, New York, 1964).
- [41] M. Bleicher, *et al.*, J. Phys. G **25**, 1859 (1999).